Accelerating the Convergence to Equilibrium of Ocean–Climate Models

KIRK BRYAN

Geophysical Fluid Dynamics Laboratory/NOAA, Princeton, NJ 08542

(Manuscript received 5 August 1983, in final form 19 January 1984)

ABSTRACT

Solutions corresponding to climatic equilibrium are usually obtained from atmospheric general circulation models by extended numerical integration with respect to time. Because the ocean contains a much wider range of time scales, the same procedure is not practical for ocean general circulation models. The ocean contains the same high frequency waves as the atmosphere and in addition, has ultra low frequencies associated with slow diffusion of water mass properties below the main thermocline. For the parameter range in which equilibrium solutions exist, a method based on distorted physics partially circumvents this difficulty. The distorted physics compresses the frequency band of the ocean model by slowing down gravity waves and speeding up abyssal processes. The acceleration of abyssal processes is accomplished by decreasing the local heat capacity without altering the transport and mixing of heat. Numerical integration of the distorted-physics ocean model then converges to equilibrium nearly as efficiently as an atmospheric model of comparable spatial resolution. Equilibrium solutions of the distorted- and nondistorted-ocean models are equivalent because the distortion only involves local derivatives with respect to time. A joint ocean–atmosphere model study provides a practical demonstration of the method.

1. Introduction

In climate research rather detailed numerical models of the atmosphere, called atmospheric general circulation models (GCMs), have proven to be extremely useful in solving many basic problems, particularly the sensitivity to small changes in radiation or external boundary conditions. However, application of these atmospheric models can only be carried up to a certain point. Basic climatic questions can only be answered by taking into consideration the entire fluid envelope of the earth, including the ocean. A reasonable question to ask is the following: Are the same numerical methods used successfully in the atmospheric GCMs also applicable to the oceans, or do they require substantial modification? The question is certainly a natural one, since the physics which govern the ocean and the atmosphere are the same. The atmosphere responds to changing external boundary conditions in less than one year. Thus it is possible to find solutions corresponding to atmospheric equilibrium by a straightforward numerical integration, similar to an extended weather forecast. In fact, the more detailed atmospheric GCMs are not unlike those used in medium range forecasting. On the other hand, the heat capacity of the ocean is more than three orders of magnitude greater than that of the atmosphere. The turnover time of ocean waters is so extremely long that the time required for the ocean to adjust to external boundary conditions is of the order of 1000 years. Since the ocean also retains many of the high frequency processes that are contained in the atmosphere, the ocean represents a broad-banded system with a frequency-range order of magnitude greater than the atmosphere. It is obviously impractical to force ocean models of even moderate spatial resolution to equilibrium by straightforward numerical integration. Estimates of computer requirements for some typical examples are given in Appendix A.

Some problems in climate can be studied by coupled models of the ocean and atmosphere without the ocean model being in equilibrium. After all, the real ocean is probably not in complete equilibrium with the present climate. At any given time the global ocean is probably heating or cooling. However, too large a departure from equilibrium in the ocean component of a climate model causes a climate "drift" which may obscure any conclusions to be drawn in a climate study. Over the years the author and his colleagues have developed an iterative method for forcing low-resolution ocean circulation models to equilibrium solutions without resorting to lengthy numerical integration of the full model. The method is based on modifying the time scales of the system to reduce the bandwidth of natural frequencies of the model by distorting the physics. A notable example of this same approach is the work of Chorin (1967) on steady-state Bénard convection. The basic idea is to find another physical system which has the same steady-state solution, but which has time-dependent properties more favorable for numerical integration to equilibrium than the original system.

The following section is devoted to defining the model and estimating the speed of ocean currents and

the velocity of gravity waves. This is followed by an analysis of the effect of the distorted physics on the dispersion of gravity waves and Rossby waves for both the extra tropics and the equatorial oceans. The modification of baroclinic instability by the distorted physics is briefly presented in another section, followed by a description of the application of the method to a specific example of a coupled ocean–atmosphere model.

The more standard approach to reducing the frequency bandwidth of models is filtering. An example is the quasi-geostrophic approximation introduced by Charney (see Pedlosky, 1979). Hasselmann (1982) has recently proposed methods for ocean climate models which involve extensive filtering, and a novel method of decoupling regions of "fast" and "slow" physics. The relationship between Hasselmann's approach and the distorted physics approach used here will be discussed in a concluding section.

2. Model equations

To fix ideas, let us set down the governing equations of an ocean model. Let $\mathbf{u}$ represent the horizontal velocity, and ∇ the horizontal gradient operator. The equations of motion with the Boussinesq assumption, and the continuity equation may be written

$$d_t\mathbf{u} + f\mathbf{k} \times \mathbf{u} + \frac{\nabla P}{\rho_0} = \mathbf{F}, \tag{2.1}$$

$$\rho g + \partial_z P = 0, \tag{2.2}$$

$$\nabla \cdot \mathbf{u} + \partial_z w = 0. \tag{2.3}$$

Here d_t is the substantive derivative, ∂_z the partial derivative with respect to z, f is the Coriolis parameter, P the pressure and ρ the density; ρ_0 is the reference density, w the vertical component of velocity, g the acceleration of gravity and $\mathbf{F}$ represents an unspecified closure approximation for smaller-scale, unresolved motions. The metric terms involving the relative angular velocity about the Earth's axis of rotation of the currents are included in atmospheric models, but can safely be neglected in ocean models.

The equation of state for sea water is a complicated expression involving potential temperature θ pressure and salinity S.

$$\rho = G(p, \theta, S). \tag{2.4}$$

It is convenient to use potential temperature as a predicted variable, rather than temperature itself to allow for the effects of compression. The predictive equations for potential temperature and salinity may be written

$$d_t\begin{pmatrix}\theta\\ S\end{pmatrix} = \begin{pmatrix}Q\\ \sigma\end{pmatrix}, \tag{2.5}$$

where Q and σ represent the closure approximations representing the effects of mixing by unresolved motions.

Let us compare the problem of finding equilibrium in ocean models with that of finding equilibrium in atmospheric models. State-of-the-art atmospheric general circulation models resolve synoptic-scale motions and contain fairly detailed models of radiation and the hydrologic cycle. As stated in the Introduction, such a model will reach equilibrium in 6 to 12 months of integration with respect to time. The heat capacity of the atmosphere is less than 1/1000 that of the ocean, while the heating anomalies driving the two systems to equilibrium are essentially the same. Thus complete equilibration of the ocean, including the deep ocean, will require from 500 to 1000 years. Radioactive tracers provide independent confirmation of these time scales.

To gauge the effort required to make straightforward numerical integration over the equivalent of 500 to 1000 years we can examine the wave and current velocities shown in Table 1. Table 1 shows that there is no real difference between the phase speeds of the external modes in the atmosphere and the ocean. If external gravity waves are fully resolved the limitations on time step would be about the same in both models. When the external gravity mode is filtered out of the ocean model, the situation is better. The time step for ocean models can be 100 times longer than that of the atmosphere, but even this advantage does not compensate for the difference of 1000 in the natural time scales.

3. Distorted physics

In order to analyze the behavior of the distorted-physics model, consider an adiabatic frictionless version of the model specified in Section 2 which is linearized about a resting basic state. Let us lump the effects of temperature and salinity together into a single variable. For convenience, let the buoyancy be defined as

$$b = \frac{-\rho g}{\rho_0}. \tag{3.1}$$

To represent the distorted physics we will introduce two parameters, α and γ, where α is a global constant and γ is a function of depth only. The equivalent of (1.1)–(1.5) is

TABLE 1. Velocities of physical phenomena which may limit the time step of a numerical integration in an atmospheric or ocean model in units of m s^{-1}.

Type	Atmosphere	Ocean
Gravity wave		
External	300	200
First internal mode	100	3
Currents		
Jets	150	1.5
Interior	—	0.2

$$\partial_t u + \frac{1}{\alpha}\left(f\mathbf{k}\times\mathbf{u} + \frac{\nabla P}{\rho_0}\right) = 0, \tag{3.2}$$

$$b - \frac{(\partial_z P)}{\rho_0} = 0, \tag{3.3}$$

$$\nabla\cdot\mathbf{u} + \partial_z w = 0, \tag{3.4}$$

$$\partial_t b + \frac{N^2 w}{\gamma} = 0. \tag{3.5}$$

In (3.5) N^2 is the Brunt–Väisälä frequency. Eqs. (3.2) and (3.5) can be restored to their usual form by introducing a stretched time and an artificial stratification. Thus (3.2) and (3.5) become

$$\partial_{t'}\mathbf{u} + f\mathbf{k}\times\mathbf{u} + \frac{\nabla P}{\rho_0} = 0, \tag{3.6}$$

$$\partial_{t'} b + N'^2 w = 0. \tag{3.7}$$

Here $t' = t/\alpha$ is a stretched time and $N'^2 = N^2\alpha/\gamma$ is a distorted stratification. The advantage of casting the equations in this form is that it then becomes possible to perform a vertical normal mode decomposition (see Moore and Philander, 1977). Expanding the velocity and pressure in terms of

$$\left(\mathbf{u}, \frac{P}{\rho_0}\right) = \sum_{n=1}^{\infty} (\mathbf{U}_n, gh_n)Z_n, \tag{3.8}$$

the normal modes Z_n of (3.2)–(3.5). Substituting (3.8) into (3.6), (3.7), (3.3) and (3.4), we obtain a set of shallow water equations for each mode.

$$\partial_{t'}\mathbf{U}_n + f\mathbf{k}\times\mathbf{U}_n + g\nabla h_n = 0, \tag{3.9}$$

$$\partial_{t'} h_n + H'_n\nabla\cdot\mathbf{U}_n = 0. \tag{3.10}$$

In the next two sections the effect of the distorted physics on the dispersion of midlatitude and equatorial waves will be analyzed on the basis of (3.9) and (3.10).

4. Midlatitude waves

Let us consider solutions to (3.9) and (3.10) of the form,

$$U_n, h_n \sim \exp[i(kx + ly - \omega' t')]. \tag{4.1}$$

In the case of a midlatitude f-plane, the dispersion relation becomes

$$\omega'^2 = f^2 + gH'_n(k^2 + l^2). \tag{4.2}$$

If we consider only the very simple case in which only α is greater than one and $\gamma = 1$ at all depths,

$$H'_n = H_n\alpha. \tag{4.3}$$

Since, in general,

$$\omega' = \omega\alpha, \tag{4.4}$$

(In principle the case of γ varying with z could be considered, but it involves finding a new set of equivalent depths, H_n, $n = 1, 2\cdots$) substitution of (4.3) into (4.2) yields

$$\omega^2 = \frac{f^2}{\alpha^2} + \left(\frac{gH_n}{\alpha}\right)(k^2 + l^2). \tag{4.5}$$

Dispersion curves in the ω–k plane for inertia–gravity waves are shown in Fig. 1 for $\alpha = 20$. The effect of large α is to reduce the frequency and lower the speed of gravity waves by a factor of $\alpha^{-1/2}$.

Since the frequencies of gravity waves and Rossby waves are well separated in midlatitudes, we can calculate the dispersion of Rossby waves for the quasi-geostrophic form of (3.9) and (3.10)

$$\partial_{t'}[\nabla^2 - (f^2/gH')]h + \beta\partial_x h = 0. \tag{4.6}$$

Substituting in the solution (4.1) we obtain,

$$-\omega' = \beta k\left(k^2 + l^2 + \frac{f^2}{gH'_n}\right)^{-1}. \tag{4.7}$$

For the case of $\gamma = 1$, (4.7) combined with (4.3) and (4.4) becomes,

$$\omega = -\beta k\left[\alpha(k^2 + l^2) + \frac{f^2}{gH_n}\right]^{-1}. \tag{4.8}$$

Equation (4.8) has an interesting asymptotic behavior. As $(k^2 + l^2) \to 0$, the effect of the distorted physics vanishes. Fig. 1 shows that for $l = 0$ the distorted and undistorted curves merge as $k \to 0$. The general effect

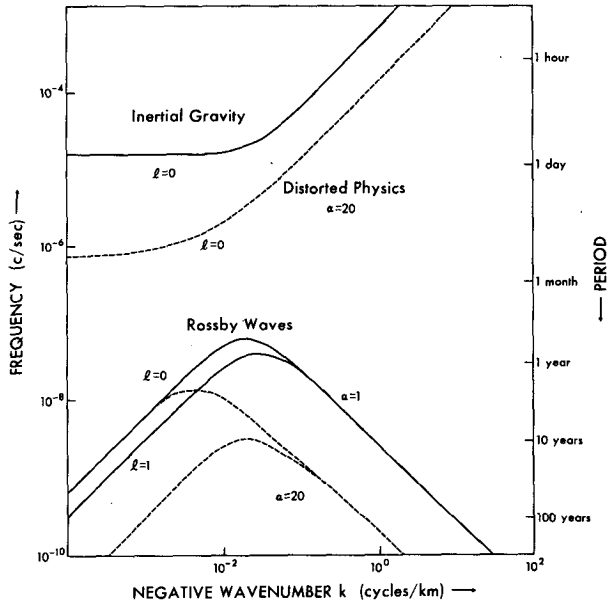

FIG. 1. Dispersion diagram for midlatitude waves corresponding to a radius of deformation of 50 km. The distortion factor α is equal to 20. Solid lines are for undistorted physics and dashed lines are for distorted physics.

of large α is to lower the frequency of Rossby waves. In addition it tends to shift the maximum frequency towards lower east–west wavenumbers.

5. Equatorial waves

Since waves at the equator have some unique properties, we extend our analysis of the distorted physics to this region. Eqs. (3.9) and (3.10) apply to an equatorial β-plane if βy is substituted for f in the Coriolis term. Moore and Philander (1977) show how the shallow water equations on the equatorial β-plane can be reduced to a single equation in the meridional velocity.

$$\partial_{t'}[gH'_n\nabla^2 - (\beta y)^2 - \partial_{t'^2}]V_n + \beta g H'_n \partial_x V_n = 0. \quad (5.1)$$

As before t' and H'_n correspond to stretched time, and the altered equivalent depth of the distorted physics. Assuming a solution to (5.1) of the form,

$$V_n = A(y)e^{i(kx-\omega' t')} \quad (5.2)$$

and defining a new meridional coordinate,

$$\eta = \beta^{1/2} y (gH'_n)^{-1/4}, \quad (5.3)$$

we obtain,

$$(d_{\eta\eta} + 2j + l - \eta^2)A = 0. \quad (5.4)$$

Solutions to (5.4) are parabolic cylinder functions with characteristic values,

$$2j + l = \frac{-(gH')^{1/2}}{\beta}\left(k^2 + \frac{k\beta}{\omega'} - \frac{\omega'^2}{gH'}\right). \quad (5.5)$$

For the case of $\gamma = l$ we make use of (4.3) and (4.4) so that (5.5) becomes

$$2j + l = -\frac{(gH\alpha)^{1/2}}{\beta}\left(k^2 + \frac{k\beta}{\omega\alpha} - \frac{(\omega\alpha)^2}{gH\alpha}\right), \quad (5.6)$$

and (5.3) becomes

$$\eta = \beta^{1/2} y (gH\alpha)^{-1/4}. \quad (5.7)$$

Hermite polynomials, to which the parabolic cylinder functions are proportional, have the property of being oscillatory near the equator in the range

$$\eta < (2j + 1)^{1/2} \quad (5.8)$$

and evanescent at higher latitudes. Relation (5.7) shows that α will change the scale of equatorial trapped waves but the ¼ power dependence on α is rather weak.

Eastward and westward propagating waves are shown in Fig. 2. For the case of $\gamma = 1$, the Kelvin wave speed is

$$C' = \sqrt{\frac{gH}{\alpha}}. \quad (5.9)$$

In the distorted physics, the speed of long Rossby waves is the same fraction of the Kelvin wave speed as in the undistorted case. All equatorially trapped waves have some meridional structure. There is no tendency for the frequencies of the distorted physics case to merge with the true physics case for low east–west wavenumbers.

6. Distorted physics and baroclinic instability

Completely aside from numerical instabilities, physical instabilities may interfere with convergence to an equilibrium solution. For this reason it is important to investigate how the distorted physics affects

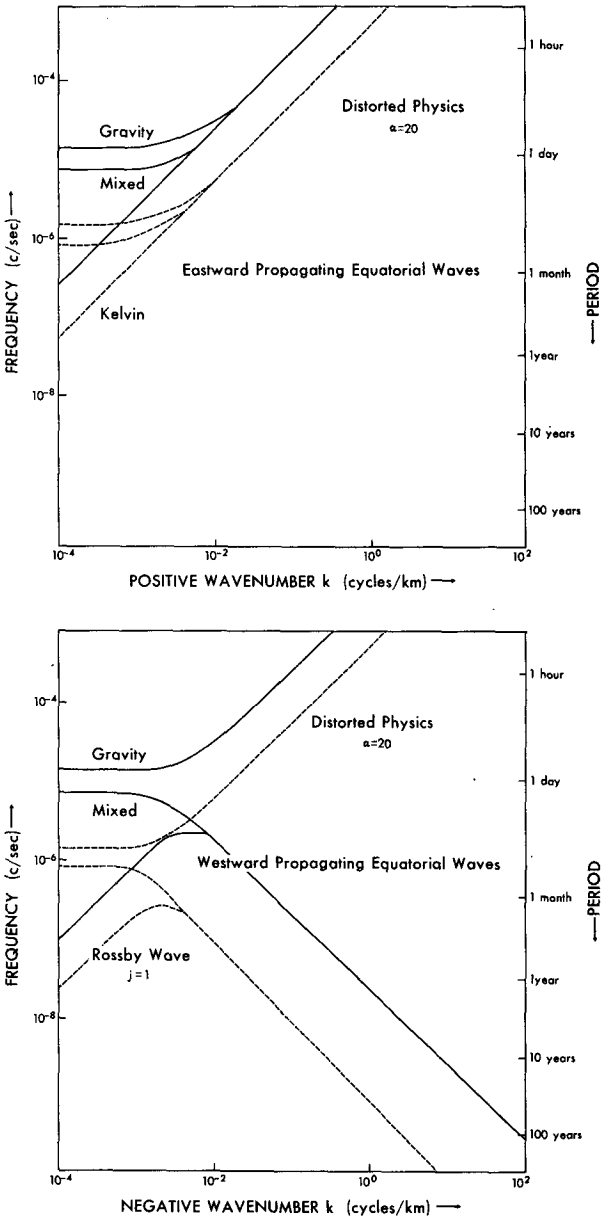

FIG. 2. Dispersion diagram for equatorially trapped waves. The equatorial radius of deformation is 50 km and the distortion factor is 20 for (upper) eastward propagating waves and (lower) westward propagating waves. Solid lines are for undistorted physics and dashed lines are for distorted physics.

baroclinic instability. To simplify the analysis we will consider a two-layer model with uniform zonal flow. The equations of a quasi-geostrophic model are

$$\alpha\partial_t\nabla^2\psi_1 + U_1\partial_x\nabla^2\psi_1 - \lambda^2(\partial_t + U_1\partial_x)(\psi_1 - \psi_2) + [\beta + \lambda^2(U_1 - U_2)]\partial_x\psi_1 = 0, \quad (6.1)$$

$$\alpha\partial_t\nabla^2\psi_2 + U_2\partial_x\nabla^2\psi_2 + \lambda^2(\partial_t + U_2\partial_x)(\psi_1 - \psi_2) + [\beta - \lambda^2(U_1 - U_2)]\partial_x\psi_2 = 0, \quad (6.2)$$

where $\lambda^2 = f_0^2/gH$, H is the thickness of both layers. These are the standard equations (Holton, 1979) except for α, the distortion factor, which appears as a coefficient of the local change of vorticity in each layer. It does not appear in the other time-derivative terms associated with vortex stretching.

Assuming solutions of the form,

$$\psi_1 = Ae^{ik(x-ct)}, \quad \psi_2 = Be^{ik(x-ct)}, \quad (6.3)$$

which do not vary in the y-direction, (6.1) and (6.2) become

$$\begin{pmatrix} a_{11} & a_{12} \\ a_{21} & a_{22} \end{pmatrix}\begin{pmatrix} A \\ B \end{pmatrix} = 0, \quad (6.4)$$

$$\left.\begin{aligned} a_{11} &= (\alpha c - U_1)k^2 + \beta + \lambda^2(c - U_2) \\ a_{12} &= -\lambda^2(c - U_1) \\ a_{21} &= -\lambda^2(c - U_2) \\ a_{22} &= (\alpha c - U_2)k^2 + \beta + \lambda^2(c - U_1) \end{aligned}\right\}.$$

Let us assume a translating coordinate system such that

$$U_1 = -U_2, \quad (6.5)$$

also let

$$U_T = \frac{1}{2}(U_1 - U_2). \quad (6.6)$$

For convenience let us define a new variable

$$\mu = \frac{k^2}{2\lambda^2}. \quad (6.7)$$

The wave speeds obtained from the characteristic values of (6.4) are,

$$c = \frac{-\beta(2\alpha\mu + 1)}{4\lambda^2\mu(\alpha^2\mu + \alpha)} \pm \delta^{1/2}, \quad (6.8)$$

$$\delta = \frac{\beta^2/\lambda^4}{16\mu^2(\alpha^2\mu + \alpha)^2} - \frac{U_T^2(1 - \mu)}{\alpha^2\mu + \alpha}. \quad (6.9)$$

Growth rates as a function of vertical shear and east–west wavenumber are shown in Fig. 3. For $\alpha = 1$, (6.8) and (6.9) reduce to the usual formulas for a two-level model (e.g., see Holton, 1979, p. 218). The effect of large α is to reduce the growth rate of baroclinically unstable waves. Thus a very small amount of friction is sufficient to damp the waves. On the other hand, the threshold shear is reduced so that instability will be present over a wider range.

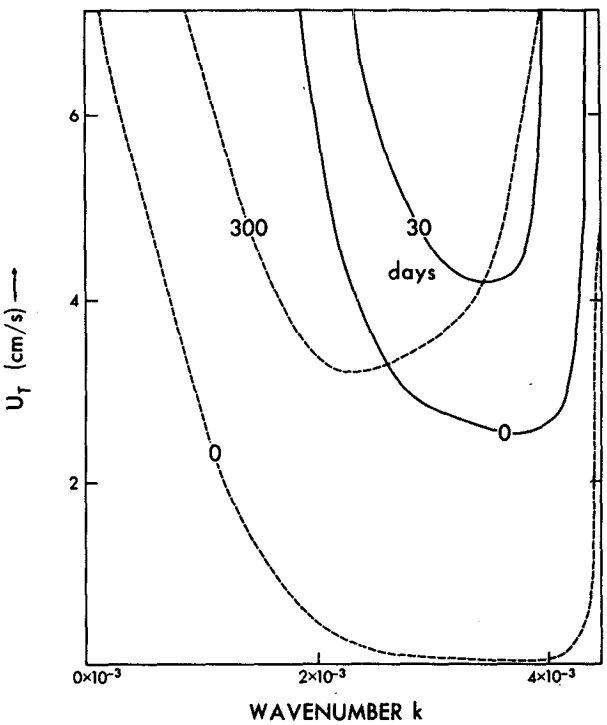

FIG. 3. Growth rate in days for two layers of equal depth. The distortion factor and radius of deformation are the same as those used in Fig. 1. Solid lines are for undistorted physics and dashed lines are for distorted physics.

7. A specific example

In the preceding sections we have analyzed the effects of the distorted physics on free waves and unstable waves. To show how the distorted physics can be applied in a specific case, we consider a recent calculation by Bryan *et al.* (1982). In order to look at the transient response of an air–sea model to a sudden increase of atmospheric CO_2, an equilibrium climate had to be computed as an initial condition. Without the application of an accelerated iterative method, a straightforward time-integration of the model would have been too lengthy to be feasible.

The ocean model of Bryan *et al.* (1982) has a simple geometry. It is enclosed between two meridians 60° of longitude apart and runs from the North pole to the equator. There are 12 levels, spaced as shown in Table 2. Horizontal resolution is 4.5° of latitude and 3.75° of longitude, with a Fourier filtering applied in the zonal direction poleward of 42°N to compensate for the convergence of meridians (see Bryan *et al.*, 1975 for details). The minimum horizontal spacing is thus the east–west distance between grid points at 42°N or about 250 km.

To insure that the advective velocity rather than a wave speed will determine the time step requires that

$$U > \sqrt{\frac{gH_n}{\alpha}} = C_{n'}, \quad (7.1)$$

TABLE 2. Time steps used in the temperature and salinity equations in the study of Bryan *et al.* (1982).

Level	Z (m)	Δt (days)	γ
1	25.5	3.0	1.00
2	81.1	3.0	1.00
3	169.5	3.0	1.00
4	295.3	3.0	1.00
5	482.8	4.6	0.65
6	754.6	11.6	0.26
7	1130.6	21.3	0.14
8	1622.4	34.4	0.09
9	2228.3	60.8	0.05
10	2934.7	73.0	0.04
11	3720.9	79.7	0.04
12	4565.5	83.0	0.04

where U is the maximum advective speed and $C_{n'}$ is the distorted speed of an internal gravity wave, the fastest wave in the system. Thus

$$\alpha_{\min} > \frac{gH_n}{U^2} \tag{7.2}$$

is a criterion for choosing α. The actual parameters are shown in Table 3. The distortion parameter α is chosen to be 2019 rather than the value of 144 based on the normal speed of the first baroclinic mode internal gravity wave speed. Table 2 shows the choice of time steps at each level. Since the advective velocity decreases with depth, it is possible to increase the time step. This allows a time step of over 80 days at the lowest level which is very useful in accelerating convergence in the deep sea.

All of the analysis of the preceding sections is based on a uniform value of γ with respect to depth. However, an increasing time step at greater depths in the temperature and salinity equations is equivalent to γ as defined in (3.5) decreasing with depth. Values are given in Table 4. In terms of the linearized equations it is obvious that an increasing time step with depth will have the same effect as increasing the stratification in deep water, changing the modal structure and internal wave speeds. As a result, internal gravity waves will move faster in the distorted physics system. To compensate for this α was chosen to be 2019 instead of the minimum value of 144 given in Table 3.

The calculations of Bryan *et al.* (1982) have recently been repeated. The coupled model is integrated for an extended period, equivalent to 6.5 years for the atmosphere and 650 years for levels 1–4. The equivalent length of integration for the deeper levels is given by the ratio of time steps shown in Table 2. The final result of this extended integration is used as an initial condition for a 50 year synchronous integration in which the time scales are uniform in the atmosphere and all levels in the ocean. There is almost no net change in average sea surface temperature. In Table 4 the net heating and cooling of the entire ocean is given for 5 year periods in units of W m^{-2}. Note that the net heating rarely exceeds 1 W m^{-2}, and the average for the entire period is less than 0.4 W m^{-2}. At this rate of heating 300 years would be required for the upper kilometer of the ocean to warm 1.0°C. This slow drift is a very small departure from complete equilibrium. The synchronous integration tests the degree of climate equilibrium obtained by the accelerated method, and the results of Table 4 show that a remarkable state of balance has been achieved.

8. Discussion

Model studies of global climate suggest that the system responds in a nearly linear fashion to small perturbations of external conditions. The equilibrium climate itself, however, may involve many highly interactive processes. This is particularly true of the climate of the ocean. As pointed out in the Introduction, straightforward numerical integration of the equations of an ocean model is not an efficient way of finding an equilibrium solution. The broad-banded character of the ocean with respect to natural frequencies makes

TABLE 3. Parameters used in the ocean model of Bryan *et al.* (1982). Stability criterion for mixing requires a factor of 1/4 because the differencing is uncentered over 2 time steps for the diffusion terms. The first-mode internal gravity wave speed is assumed to be 3 m s^{-1}.

Parameter	Symbol	Value	Maximum time step: Formula	Maximum time step: Value (days)
Minimum horizontal spacing	Δx	250 km	—	—
Minimum vertical spacing	Δz	50 m	—	—
Minimum possible distortion factor	gH'/U^2	144	—	—
Actual distortion factor	α	2019	—	—
Horizontal diffusion	A_{HH}	10^3 m^2 s^{-1}	$\Delta t < (\Delta x)^2/4A_{HH}$	181
Horizontal viscosities	A_{HM}	2.5×10^5 m^2 s^{-1}	$\Delta t < (\Delta x)^2/4A_{HM}$	1462
Vertical diffusion	A_{VH}	0.3×10^{-4} m^2 s^{-1}	$\Delta t < (\Delta z)^2/4A_{VH}$	241
Vertical viscosity	A_{VM}	20.0×10^{-4} m^2 s^{-1}	$\Delta t < (\Delta z)^2/4A_{VM}$	7300
Maximum velocity	U	0.25 m s^{-1}	$\Delta t < \Delta x/2U$	5.8

TABLE 4. Results from a numerical integration of a coupled atmosphere-ocean model of Bryan *et al.* (1982). Net surface heating of the ocean is shown for synchronous integration to test the climatic equilibrium obtained by using multiple time scales.

Time interval (years)	Average ocean surface heating (W m^{-2})
0–5	0.42
5–10	0.38
10–15	1.06
15–20	1.22
20–25	0.06
25–30	−0.02
30–35	0.25
35–40	−0.08
40–45	0.35
45–50	0.40
50 year average	0.40

it necessary to resolve a range of time scales three orders of magnitude greater than that for the atmosphere. The distorted physics approach, which has been used in a large number of ocean climate studies, attempts to narrow the frequency band of ocean models in two ways. Gravity waves and Rossby waves are decreased in speed in such a way that equilibrium solutions are unchanged. This eliminates the very high frequencies. At the same time the very long time scales are reduced by shrinking the local time scale of the deep sea relative to the upper ocean. This distortion may also be interpreted as decreasing the local heat and salt capacity of the deep ocean without altering the advective or diffusive fluxes of these quantities. Since only local derivatives with respect to time are changed, equilibrium solutions with distorted physics should correspond exactly to equilibrium solutions for the prototype model. High resolution models in a parameter range which allows baroclinically unstable disturbances cannot, of course, be handled in this way.

Recently, Hasselmann (1982) has outlined methods for addressing the same problem. His approach is based on drastic filtering to remove both gravity waves and short Rossby waves. In addition, Hasselmann (1982) proposes to use a "mosaic" of separate models for different regions of the ocean which would isolate the "fast" physics of boundary regions from the "slow" physics of the ocean interior. The regional models would be coupled in a non-synchronous fashion to provide the required fluxes between the different regions. There is an analogy between the use of different time scales in the horizontal plane as suggested by Hasselmann (1982), and the use of different time scales in the vertical plane outlined in this paper. Future work should be directed to determining if the best features of Hasselmann's (1982) methods and the distorted physics approach can be combined to form an even more efficient method of calculating ocean climate.

Acknowledgments. The author is very grateful to Mr. Michael Cox, Mr. Michael Spelman and Professor Toshio Yamagata for comments, and to Mrs. Elizabeth Williams and Miss Martha Jackson for assistance in preparing the manuscript. The author would also like to thank Mr. Philip Tunison and his staff for preparing the drawings.

APPENDIX A

Machine Requirements

The vectorization of arithmetic operations in modern large scale computers makes it very difficult to predict machine requirements on the basis of experience on a different piece of equipment. Just to provide a concrete example, Fig. A1 shows the convergence of a primitive equation, World Ocean model with fixed surface boundary conditions specified from observations. The model is similar to that of Case I (low resolution) of Bryan and Lewis (1979). Initially the temperature and salinity are uniform in both horizontal and vertical directions. Within 20 000 iterations convergence is virtually complete. The time steps parameters correspond exactly to those of Table 2 and 3. Based on the 3-day time step at upper levels, 20 000 iterations is equivalent to an integration of 164 years. For an 80 day time step at lower levels, the same number of iterations is equivalent to over 4 000 years of integration.

A spectral model of the atmosphere with approximately the same horizontal and vertical resolution and

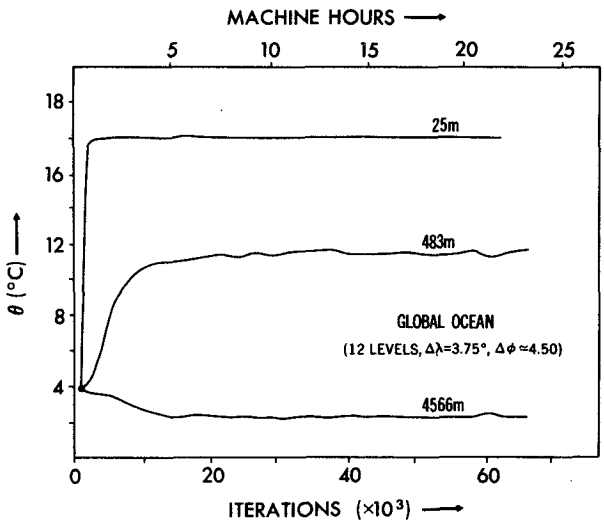

FIG. A1. Area-averaged potential temperature in a model of the World Ocean. The trend of temperature as a function of the number of iterations is a measure of the convergence of the accelerated method. The model is similar to Bryan and Lewis (1979).

using an implicit method with respect to gravity waves requires 5–6 hours of CYBER 205 machine time, and approximately 18 000 iterations. Thus it takes about the same amount of computational effort to reach equilibrium for an ocean model with the distorted physics and compressed time scales as it does to integrate over one year in an atmospheric model of comparable resolution.

REFERENCES

Bryan, K., S. Manabe and R. L. Pacanowski, 1975: A global ocean–atmosphere climate model. Part II: The oceanic circulation. *J. Phys. Oceanogr.*, **5**, 30–46.

——, and L. J. Lewis, 1979: A water mass model of the world ocean. *J. Geophys. Res.*, **84**, 2503–2517.

——, F. G. Komro, S. Manabe and M. J. Spelman, 1982: Transient climate response to increasing atmospheric carbon dioxide. *Science*, **215**, 56–58.

Chorin, A. J., 1967: A numerical method for solving incompressible viscous flow problems. *J. Comp. Phys.*, **2**, 12–26.

Hasselmann, K., 1982: An ocean model for climate variability studies. *Progress Oceanography*, Vol. 11, Pergamon, 69–92.

Holton, J. R., 1979: *An Introduction to Dynamic Meteorology*, 2nd ed., Academic Press, 391 pp.

Moore, D., and S. G. H. Philander, 1977: Modelling of the tropical oceanic circulation. *The Sea*, Vol. 6, Wiley, 319–361.

Pedlosky, J., 1979: *Geophysical Fluid Dynamics*, Springer-Verlag, 624 pp.